JCIM JOURNAL OF CHEMICAL INFORMATION AND MODELING
Cite This: J. Chem. Inf. Model. XXXX, XXX, XXX−XXX
Article
pubs.acs.org/jcim

Exploring Gatekeeper Mutations in *EGFR* through Computer Simulations

Srinivasaraghavan Kannan,*,† Stephen J. Fox,† and Chandra S. Verma*,†,‡,§

†Bioinformatics Institute, Agency for Science Technology and Research (A*STAR), 30 Biopolis Street, #07-01 Matrix, Singapore 138671 Singapore

‡School of Biological Sciences, Nanyang Technological University, 60 Nanyang Drive, Singapore 637551, Singapore

§Department of Biological Sciences, National University of Singapore, 14 Science Drive 4, Singapore 117543, Singapore

Supporting Information

ABSTRACT: The emergence of resistance against drugs that inhibit a particular protein is a major problem in targeted therapy. There is a clear need for rigorous methods to predict the likelihood of specific drug-resistance mutations arising in response to the binding of a drug. In this work we attempt to develop a robust computational protocol for predicting drug resistant mutations at the gatekeeper position (T790) in *EGFR*. We explore how mutations at this site affects interactions with ATP and three drugs that are currently used in clinics. We found, as expected, that certain mutations are not tolerated structurally, while some other mutations interfere with the natural substrate and hence are unlikely to be selected for. However, we found five possible mutations that are well tolerated structurally and energetically. Two of these mutations were predicted to have increased affinity for the drugs over ATP, as has been reported earlier. By reproducing the trends in the experimental binding affinities of the data, the methods chosen here are able to correctly predict the effects of these mutations on the binding affinities of the drugs. However, the increased affinity does not always translate into increased efficacy, because the efficacy is affected by several other factors such as binding kinetics, competition with ATP, and residence times. The computational methods used in the current study are able to reproduce or predict the effects of mutations on the binding affinities. However, a different set of methods is required to predict the kinetics of drug binding.

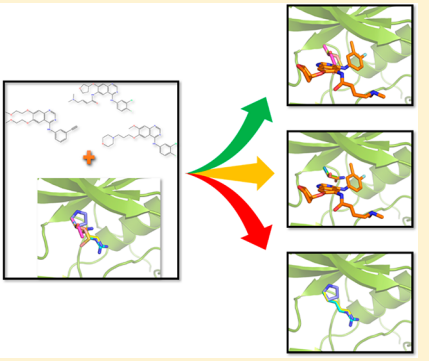

INTRODUCTION

Kinases catalyze the transfer of a phosphate group from ATP to Ser, Thr, and Tyr residues in numerous protein substrates, thereby activating multiple signaling pathways. This implicates them in all aspects of cellular functions, and hence their deregulation has been implicated in numerous human diseases.[1] Targeting kinases with small molecules directed at their well characterized ATP binding pockets, or more recently, allosteric pockets, has resulted in several therapeutic successes.[2−6] They are the second-largest drug target family, with 38 approved kinase inhibitors (KI) drugs, and several are in development or clinical trials.[4−6] Most approved inhibitors are ATP-competitive and bind the ATP pocket in the active form of the kinase (these are referred to as the type I inhibitors) or straddle the ATP pocket and an adjacent allosteric pocket accessible only in the inactive form of the kinase (these are referred to as the type II inhibitors). Since all kinases share very similar features in their ATP-binding pockets, selectivity becomes a major problem. In addition, some ATP pocket residues are found to easily mutate, resulting in drug resistance.

The most common changes associated with resistance are point mutations within the kinase domain, which decrease the affinity of the kinases for the inhibitors. Some mutations may occur in the vicinity of the binding site, resulting in conformational changes that can occlude inhibitor binding, while some others can occur distal to the binding sites but inhibit binding allosterically.[7−10] Various approaches have been used to discover such resistance causing mutations for the discovery of new inhibitory molecules that can accommodate the mutations.[7,11,12] These studies usually focus on a small set of clinically reported mutations. What is needed is a set of rigorous methods that can explore the full mutational spectrum possible at a position of interest and then predict which mutations are likely to be seen in the clinic.

For resistance, a mutation must result in a reduction in the affinity of the drug relative to that for ATP and catalysis should take place. Clinical studies have unveiled mutational hot spots such as the "gatekeeper mutations" within the kinase domain.[13,14] The commonly observed "gatekeeper" residue is located adjacent to the ATP binding site. It generally does not interact directly with ATP and yet engages in crucial contacts with type 1 and type 2 ATP binding site inhibitors. While it is not strictly conserved, it is the most frequent clinically observed mutation that results in drug resistance in several

Received: April 29, 2019
Published: May 17, 2019

DOI: 10.1021/acs.jcim.9b00361
J. Chem. Inf. Model. XXXX, XXX, XXX−XXX

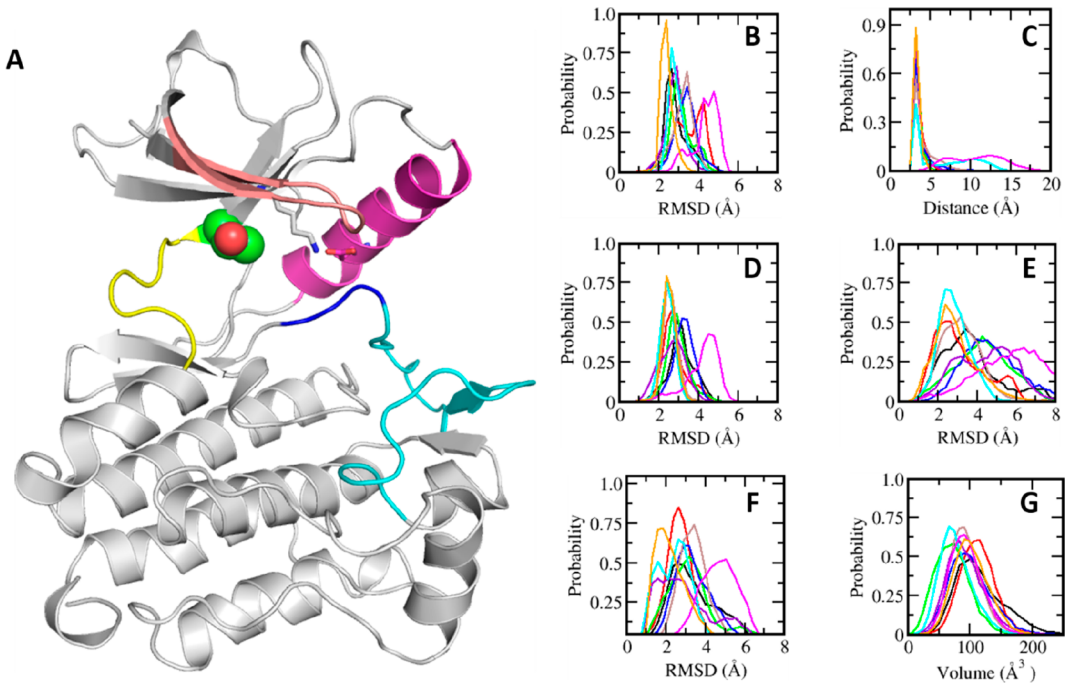

Figure 1. Overview of the structure of $EGFR^{WT}$ kinase in its active form, with the helix αC adopting the αC−In (active, magenta) and the activation loop (cyan) P-loop (salmon), Hinge (yellow), and DFG motif (blue). The gatekeeper residue T790 is shown as sphere (green) and critical residues (K745 and E762) that make the salt bridge (in magenta dashes) in the active state are shown as sticks and the salt bridge interaction is shown as red dashes. Probability distributions of the (B) root-mean-square deviation (RMSD) of the kinase domain (C) distance between the K745 and E762 salt bridge (D) RMSD of A-loop (E) RMSD of P-loop (F) RMSD of αC-helix (G) volume of the ATP pocket calculated from conformations sampled during the MD simulations of $EGFR^{WT}$ (black), $EGFR^{T790A}$ (red), $EGFR^{T790N}$ (green), $EGFR^{T790R}$ (blue), $EGFR^{T790I}$ (brown), $EGFR^{T790K}$ (violet), $EGFR^{T790M}$ (cyan), $EGFR^{T790P}$ (magenta), and $EGFR^{T790S}$ (orange).

kinases (*BCR-ABL*,[15] *EGFR*,[16] *KIT*,[17] *PDGFRα*,[18] and *Flt3*[19]). Mutations can either sterically occlude the inhibitors through small to large changes in the side chain volumes or can lose critical contacts with the inhibitors through large to small side chain changes. The T315I gatekeeper mutation in *BCR-ABL* is an example of the former (both steric clash and loss of critical h-bond) while the F691L gatekeeper mutation in *Flt3* kinase is an example of the latter resulting in the loss of stacking interactions.[15,19] The gatekeeper mutation T790M in *EGFR* results in resistance to an inhibitor by an increase in its affinity for ATP.[20]

In this work we attempt to develop a robust computational protocol for predicting resistance by asking a simple question: what are the consequences of mutating the gatekeeper Thr790 in *EGFR* to all possible amino acids (we hypothesize that only single nucleotide changes are allowed). Of the 19 possible mutations, 8 result from single base changes and are the focus of our study. We explore the binding of ATP and three drugs (gefitinib, erlotinib and afatinib), all of which bind to the active form of the kinase, in the context of the wild type (WT) and the 8 mutations at T790, using a combination of extensive molecular dynamics (MD) simulations with rigorous free energy calculations (thermodynamic integration (TI) and free energy perturbation (FEP)). It has been speculated that the T790M mutation in *EGFR* shifts the conformational equilibrium of *EGFR* from the inactive to the active state,[21−26] thus making it constitutively active.

METHODS

MD Simulations. Systems used in this current study are taken from our previous work.[26] Each system was subject to MD simulations which were carried out with the *pmemd.CUDA* module of the program Amber16.[27] All atom versions of the Amber 14SB force field (ff14SB)[28] and the general Amber force field (GAFF)[29] were used for the protein and the inhibitors, respectively. Parameters for gefitinib, erlotinib and affatinib were derived using the antechamber module of Amber 16. Gefitinib and erlotinib are noncovalently bound to *EGFR* while afatinib is covalently linked to Cys797 of *EGFR*. All MD simulations, analysis including the binding energy calculations were carried out as discussed in our previous study[26,30] and are summarized in the Supporting Information.

Prediction of Protein Stability. We used five different structure-based protein stability programs available (DUET,[31] SDM,[32] mCSM,[33] DynaMut,[34] and iStable[35]) to predict the effects of the mutations on the stability of the *EGFR* kinases. The change in protein stability (ΔΔ*G*) was computed for both the active and inactive forms of the kinases.

RESULTS

Conformational Dynamics of the *EGFR* Gatekeeper Mutations in the Apo State. We focus on the mutations that are likely to result in resistance, i.e., those that bind ATP with higher affinity than they do the inhibitory ligands and will preferentially adopt the active state in order to engage in phosphate transfer (catalysis). Therefore, we focus on $EGFR^{WT}$ and its mutants ($EGFR^{T790A}$, $EGFR^{T790R}$, $EGFR^{T790N}$, $EGFR^{T790M}$, $EGFR^{T790K}$, $EGFR^{T790I}$, and $EGFR^{T790S}$). Structurally, all of them were stable in their apo forms during the MD simulations, not deviating by more than 4 Å from their starting conformations (Figure 1B), apart from $EGFR^{T790P}$, which is not

DOI: 10.1021/acs.jcim.9b00361
J. Chem. Inf. Model. XXXX, XXX, XXX−XXX

Table 1. Effects of Mutations on the Stability of EGFR Kinase Variants Predicted Using Available Web Servers[a]

	active					inactive				
mutation	SDM	DynaMut	DUET	mCSM	iStable	SDM	DynaMut	DUET	mCSM	iStable
T790A	−0.5	−1.1	−0.5	−0.9	−1.1	−0.5	−1.2	−0.4	−0.9	−0.8
T790N	−0.5	−0.3	−1.2	−1.4	0.9	−0.4	−0.6	−0.8	−1.1	0.7
T790M	−0.3	1.0	0.2	0.1	0.1	0.1	1.4	0.3	−0.1	0.1
T790I	0.8	0.9	0.7	−0.01	0.01	0.8	0.7	0.8	−0.3	0.1
T790S	−0.8	−0.3	−1.6	−1.5	0.6	−0.6	−0.9	−1.2	−1.3	0.5

[a]Values reported here are changes in protein stability ($\Delta\Delta G$) and are classified as predicted to be neutral ($-1.5 < \Delta\Delta G < 1.5$), stabilizing ($\Delta\Delta G > 1.5$), or destabilizing ($\Delta\Delta G < -1.5$).

surprising given that the Pro introduces a distortion in the form of a kink.

Key structural elements of kinases are known to be crucial for their conformational stabilities and functional interactions with ATP[36,37] and include the αC- helix, P-loop, A-loop, and a DFG motif which is located at the N-terminal end of the A-loop and is crucial for the kinase adopting a catalytically competent state (Figure 1A). These regions are also known to undergo large conformational changes during the transitions between the active and inactive states of the kinase.[36,37] The αC-helix regulates the activity of the kinases by adopting αC-In (active) and αC-Out (inactive) conformations. It contains a conserved glutamic acid (Glu762) which forms a catalytically important salt bridge with Lys745 in the active conformation of the kinase. During the simulations, the kinases maintain their starting active states and all mutants except the $EGFR^{T790P}$ show a stable αC-In conformation including the salt bridge (Lys745−Glu762); $EGFR^{T790P}$ shows increased fluctuations of the αC helix (Figure 1F) and concomitant loss of the salt bridge (Figure 1C). The Glycine rich P-loop can adopt both closed and extended conformations, depending on whether the kinase is bound with a ligand or not. In the apo states, the P-loop is known to be highly flexible (density is often missing in crystal structures) and is seen to be very flexible in the simulations of $EGFR^{T790R}$, $EGFR^{T790N}$, $EGFR^{T790K}$, and $EGFR^{T790P}$, with the $EGFR^{T790P}$ exhibiting the largest flexibility (Figure 1E). The DFG-motif adopts a stable DFG-In conformation in all the simulations except in $EGFR^{T790P}$ where it is very flexible (Figure 1D).

We next measured the volume of the active site pocket. The $EGFR^{WT}$ has a pocket volume of ∼100 Å^3, while most mutants have pockets with volumes close to ∼100 Å^3 (Figure 1G). In the case of $EGFR^{T790A}$, the reduction in side chain results in a slightly larger pocket volume (∼120 Å^3). In contrast, the larger side chains in $EGFR^{T790K}$ and $EGFR^{T790R}$ result in somewhat smaller pockets, with volumes ∼70 Å^3; the kink in $EGFR^{T790P}$ results in a smaller pocket (volume ∼60 Å^3).

Given that all mutations except $EGFR^{T790P}$, $EGFR^{T790K}$, and $EGFR^{T790R}$ are structurally well tolerated, we investigated the effect of these mutations on the stability of the kinases. We have used structure based and MD based free energy methods to predict whether a given mutation will stabilize or destabilize the structure of *EGFR* kinase. The change in protein stability ($\Delta\Delta G$) were computed for both the active and inactive forms of the kinases. Overall the effect of these mutations on the stability of the kinases was minimal (only 10 out of the 50 $\Delta\Delta G$ values computed were predicted to stabilize/destabilize by ∼1 kcal/mol) [Table 1]. All structure-based methods predicted that mutations $EGFR^{T790M}$ and $EGFR^{T790I}$ stabilize both the active and inactive forms of the kinases, whereas $EGFR^{T790A}$, $EGFR^{T790N}$, and $EGFR^{T790S}$ are predicted to destabilize the structures.

Conformational Dynamics of the *EGFR* Gatekeeper Mutations in the ATP-Bound State. We next investigated the ability of the kinases to bind ATP. Models of the ATP complexes were generated based on the crystal structure of the $EGFR^{WT}$-AMPMP complex (PDB ID 2ITX) and subjected to MD simulations. In contrast to the apo simulations, increased structural stability (by 1−2 Å) was observed; this is not surprising as the presence of ATP is known[36,37] to stabilize the active conformation of the *EGFR* kinase (Figure 2B). The

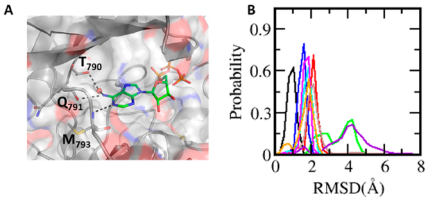

Figure 2. (A) Structure of the $EGFR^{WT}$ kinase (surface representation) in its active form bound with ATP (green sticks). Bound water molecule is shown as sphere (red) and h-bonds are highlighted (dashed lines) (B) Probability distributions of the root-mean-square deviation (RMSD) of bound ATP calculated from conformations sampled during the MD simulations of $EGFR^{WT}$ (black), $EGFR^{T790A}$ (red), $EGFR^{T790N}$ (green), $EGFR^{T790R}$ (blue), $EGFR^{T790I}$ (brown), $EGFR^{T790K}$ (violet), $EGFR^{T790M}$ (cyan), $EGFR^{T790P}$ (magenta), $EGFR^{T790S}$ (orange).

bound conformation of the ATP remained stable in all of the simulations (Figure 2B). The crystal structure (PDB ID 2ITX) shows that the adenine moiety from AMPMP (ATP analogue) is involved in h-bond interactions with the side chain of Thr790 and backbone atoms of Gln791 and Met793 (Figure 2A). The 6-amine of the adenine moiety engages the hydroxyl side chain of Thr790 and carbonyl backbone of Gln791 with hydrogen bonds. The N1 from the purine group of adenine forms an h-bond with the amide backbone of Met793. These h-bonds were well preserved during the simulations of the $EGFR^{WT}$-ATP complex. In addition we found a water mediated interaction between the 6-amine of the adenine moiety of ATP and the hydroxyl side chain of Thr790 (∼95% of the simulation). In the case of the mutants, this water is not retained; however, despite the loss of the water mediated h-bond (between the bound ATP and the side chain hydroxyl of Thr790), the bound conformation of ATP was well retained, mainly with the help of the other two h-bonds that ATP makes with the hinge region of the kinase. This suggests that this water-mediated interaction may not be critical.

In $EGFR^{T790A}$, not only was the h-bond lost, but a slight increase in flexibility of ATP was observed with average rmsd

DOI: 10.1021/acs.jcim.9b00361
J. Chem. Inf. Model. XXXX, XXX, XXX−XXX

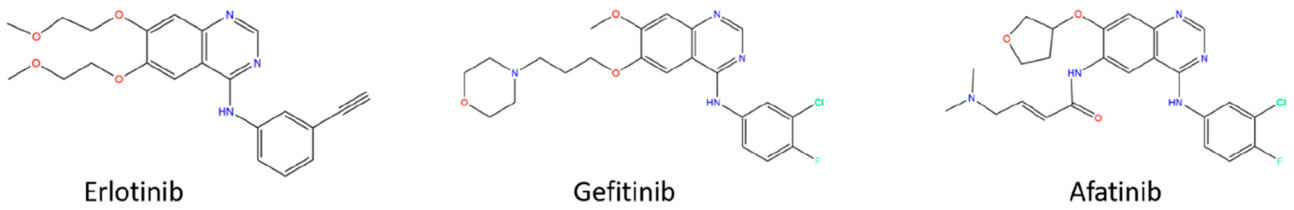

Figure 3. Structures of the three drug molecules used in this study.

of 1.9 Å (Figure 2B) due to the shorter mutant side chain; however, it still retained the binding of ATP. In the case of $EGFR^{T790M}$, the branched side chain of threonine is substituted with a longer but linear side chain residue methionine. Despite the loss in the water mediated side chain h-bond interaction made with the hydroxyl of Thr (which resulted in a slight increase in ATP rmsd to ∼1.8 Å; Figure 2B), the longer side chain of Met provides a tighter packing with the adenine moiety of the ATP; this is also seen for the longer branched side chain of Ile in $EGFR^{T790I}$ (increase in ATP rmsd to ∼2.0 Å) (Figure 2B). The observation[20] that $EGFR^{T790M}$ binds ATP with a higher affinity $EGFR^{WT}$ suggests that the water mediated interaction may not be critical. In $EGFR^{T790N}$, asparagine is similar to Ile in terms of size/length but has an amide facing the ATP and engages in water mediated interactions (∼60% of simulation time) with the amine of the adenine moiety of ATP (observed in the case of $EGFR^{WT}$), stabilizing the bound ATP with an average rmsd of 1.3 Å (Figure 2B). In the case of serine at the gatekeeper position, despite lacking the methyl group of T790, a water mediated h-bond interaction (∼85% of simulation time) with the amine of the adenine moiety in ATP is seen (as in T790). The water mediated h-bond along with the h-bond interactions with the carbonyl backbone of Gln791, and amide backbone of Met793, stabilizes the bound form of ATP as in the $EGFR^{WT}$ with average rmsd (ATP) of ∼1.1 Å (Figure 2B). As expected, the substitution of Thr with longer side chain residues such as Lys and Arg interfere with the binding of ATP with rmsd (ATP) 3.5 Å to 4.5 Å for conformations sampled during the MD simulations (Figure 2B), resulting in the displacement of the ATP to a new and noncanonical binding mode. The bound ATP also loses its hydrogen bond interactions with the hinge region. In this mode the positively charged side chain of the gatekeeper residue is attracted toward the phosphate group of ATP; this likely prevented any unbinding events during the simulations. No unbinding of ATP was observed even when the simulations were extended to 1 μs (data not shown). The Proline substitution in $EGFR^{T790P}$, introduces a kink at the gatekeeper position resulting in loss of both packing and h-bond interactions with the bound ATP; again, an increase in rmsd (ATP) of 2.1 Å (Figure 2B) was observed for the bound ATP, however no unbinding was observed.

It is clear that all of the substitutions except $EGFR^{T790P}$, $EGFR^{T790R}$, and $EGFR^{T790K}$ retain the two h-bond interactions that the ATP makes with the hinge region of the kinase in the $EGFR^{WT}$; $EGFR^{T790S}$ retains all the h-bond interactions seen in $EGFR^{WT}$. Hence it is puzzling that only the $EGFR^{T790M}$ mutation is observed in clinics. Earlier, Azam et al.[13] demonstrated experimentally that in a range of kinases, indeed the gatekeeper position was quite tolerant of various substitutions, including $EGFR^{T790I}$ and $EGFR^{T790M}$ which retain or enhance the kinase activity. Additionally, the gatekeeper threonine was found to be tolerant to substitutions with smaller side chains such as alanine in most of the cases. What was surprising was that long chains such as lysine were also well tolerated, albeit with reduced kinase activity. However, substitution to proline, which is expected to result in a kink in the polypeptide backbone at the hinge region, resulted in inactivation of the enzyme.

Conformational Dynamics of the *EGFR* Gatekeeper Mutations in the Inhibitor-Bound State. We next investigate the binding of three small molecule clinical kinase inhibitors to these mutants. These include two reversible inhibitors (gefitinib, erlotinib) and one irreversible inhibitor (afatinib) (Figure 3). Models of these inhibitors bound to the kinases were generated using the available crystal structures of the molecules bound to the $EGFR^{WT}$ kinase. All three molecules are quinazoline derivatives, bind to *EGFR* in a similar manner in the ATP pocket, and interact with the hinge region of the kinase through similar h-bond interactions: the quinazoline N1 nitrogen interacts with the amide backbone of Met793 from the hinge region and the quinazoline N3 nitrogen interacts with the hydroxyl side chain of Thr790 through a water molecule W1 (Figure 4A–C) which is conserved in most crystal structures. All inhibitors carry different solubilizing groups that protrude toward the entrance of the ATP pocket; afatinib carries an electrophile that forms a covalent bond with Cys797. The inhibitors contain phenyl derivatives (3-chloro-4fluoro–phenylamino in gefitinib and afatinib and 3-ethnylphenylamino in erlotinib) that protrude toward the back pocket of the kinase. The MD simulations of the inhibitors bound to $EGFR^{WT}$ show them to be stably

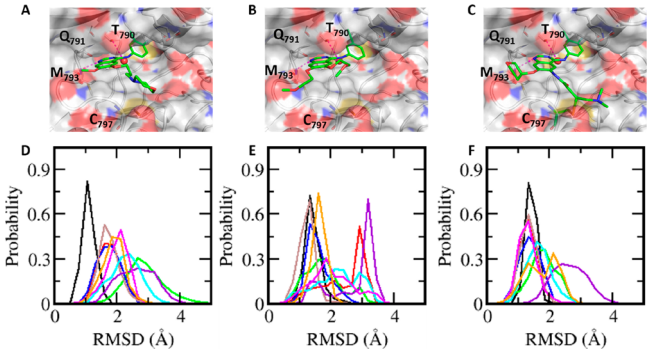

Figure 4. Structure of the $EGFR^{WT}$ kinase (surface representation) in its active form bound with (A) erlotinib (green sticks), (B) gefitinib, and (C) afatinib. Bound water molecule is shown as a sphere (red) and h-bonds are highlighted (dashed lines). Probability distributions of the root-mean-square deviation (RMSD) of bound (D) erlotinib, (E) gefitinib, and (F) afatinib calculated from conformations sampled during the MD simulations of $EGFR^{WT}$ (black), $EGFR^{T790A}$ (red), $EGFR^{T790N}$ (green), $EGFR^{T790R}$ (blue), $EGFR^{T790I}$ (brown), $EGFR^{T790K}$ (violet), $EGFR^{T790M}$ (cyan), $EGFR^{T790P}$ (magenta), and $EGFR^{T790S}$ (orange).

DOI: 10.1021/acs.jcim.9b00361
J. Chem. Inf. Model. XXXX, XXX, XXX−XXX

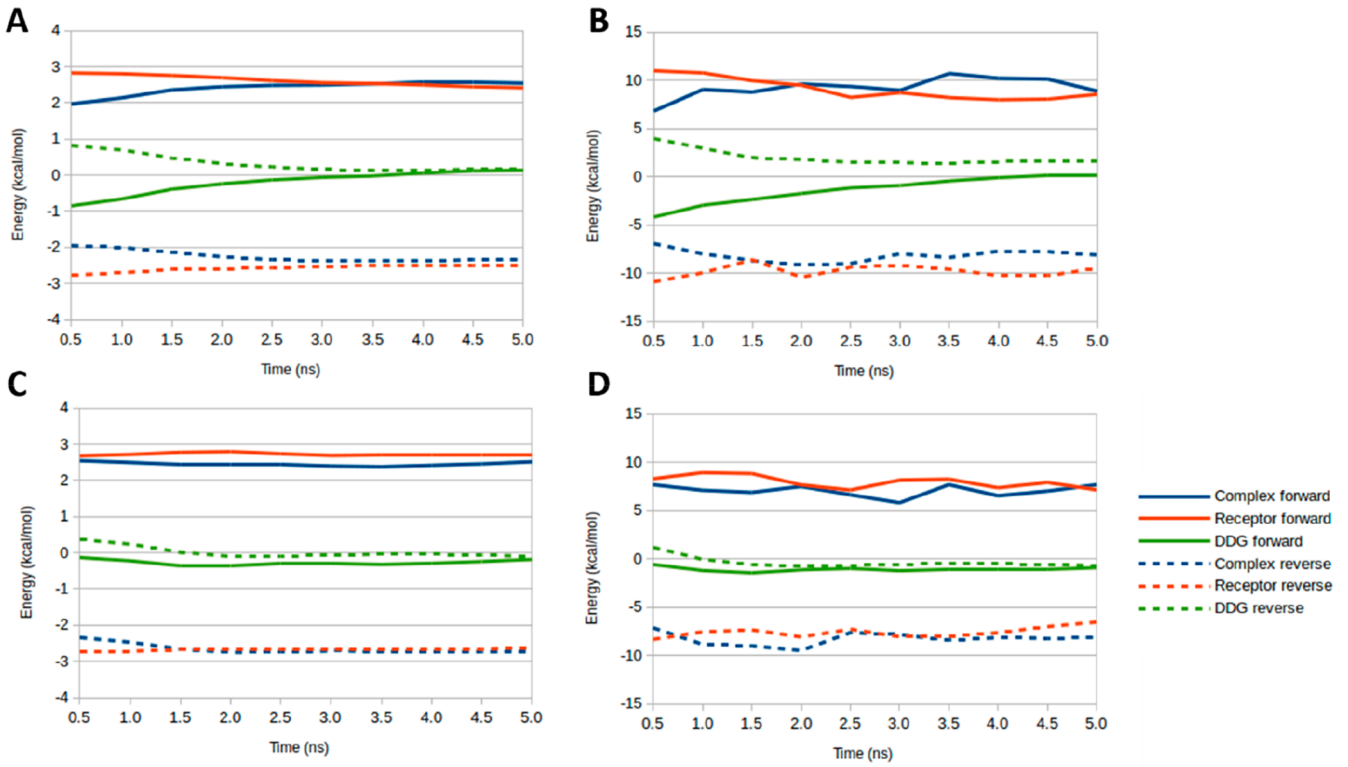

Figure 5. Convergence of the binding free energy calculations. Block averages of the (A, C) FEP/MBAR and (B, D) TI results from the forward and backward simulations for (A, B) $EGFR^{T790I}$ and (C, D) $EGFR^{T790M}$ mutants.

bound (average rmsd of 0.8, 1.7, and 2.6 Å for afatinib, erlotinib, and gefitinib, respectively, Figure 4).

Afatinib is most stable on account of its covalent linkage to the enzyme. The larger flexibility of gefitinib arises from the long and exposed solubilizing group which is not involved in any direct interactions with the kinase. The h-bond interactions between the quinazoline N1 nitrogen and amide backbone of Met793 from the hinge region and the water mediated h-bond interactions with the quinazoline N3 nitrogen and hydroxyl side chain of gatekeeper Thr790 are well preserved (~90% of the simulation time) for all inhibitors during the simulations.

We next investigate how the various mutants influence the binding of these three inhibitors during the MD simulations. Erlotinib bound stably to most of the gate keeper substitutions with its rmsd between 1.3 and 2.8 Å (Figure 4D); the hydroxyl side chain of Ser790 enables the retention of the key water mediated h-bond interactions with the bound erlotinib (Figure 4D). In the other mutants, the water molecule is displaced. Although no unbinding was observed (even with simulations extended to 1 μs) in $EGFR^{T790K}$ or $EGFR^{T790R}$, erlotinib undergoes conformational changes, especially at its amino-phenyl moiety, to accommodate the longer side chains of the mutants. Gefitinib also shows the same effects as erlotinib; the larger RMSD (~3.5 Å; Figure 4E) arises from the increased flexibility of the long and flexible solubilizing group as was also seen in $EGFR^{WT}$. The longer side chains of $EGFR^{T790R}$ and $EGFR^{T790K}$ are less tolerant, while $EGFR^{T790S}$ is the only mutant that retains the water mediated h-bond. The h-bond interactions with the hinge region of the mutant kinases are also retained except in $EGFR^{T790R}$ and $EGFR^{T790K}$ where gefitinib undergoes conformational changes; again, no unbinding was observed even with simulations extended to 1 μs.

The interactions of afatinib are also similarly influenced, with the retention of hinge interactions while the water mediated interaction was retained only by $EGFR^{T790S}$; the reduced fluctuations arise from its covalent linkage (Figure 4F). Again, the $EGFR^{T790K}$ and $EGFR^{T790R}$ side chains perturb its conformation and hence the interactions. In summary, the binding of these three drugs are well tolerated structurally with most of the mutations except for $EGFR^{T790P}$, $EGFR^{T790K}$, and $EGFR^{T790R}$ at the gatekeeper position.

Once again, it is clear that except perhaps for the $EGFR^{T790P}$, $EGFR^{T790K}$, and $EGFR^{T790R}$ mutants, the other mutants are quite tolerant and will bind ATP and the inhibitors. Next, we explore the energetic consequences of the mutations upon the binding of the ligands using free energy methods.

Effects of the EGFR Gatekeeper Mutations on the Binding Energies of ATP and Inhibitors. Thermodynamic integration (TI) and free energy perturbation (FEP) calculations performed in explicit solvent describe a thermodynamically complete picture of binding and have been shown to produce affinities in close agreement with experiments.[38−45] However, due to issues of computational costs and hence incomplete sampling, convergence has been a major issue with the regular TI and FEP calculations. To overcome this limitation, various modifications have been proposed including free energy perturbation/replica exchange with solute tempering (FEP/REST),[46] replica exchange free energy perturbation (RE-FEP)[47] and replica exchange thermodynamic integration RE-TI.[48] In addition, advanced analysis methods such as MBAR[49,50] have also been proposed to improve convergence. All of these methods have been

DOI: 10.1021/acs.jcim.9b00361
J. Chem. Inf. Model. XXXX, XXX, XXX−XXX

shown to improve convergence and to reproduce the experimental binding data with high accuracy (within ∼1 *k*T).

Binding energies were estimated by two TI and FEP based calculations: one was performed on apo *EGFR* and the other on the *EGFR*-inhibitor/ATP complex. The difference in binding energy upon mutation was computed using a thermodynamic cycle (more details in the Supporting Information). Multistate Bennett Acceptance Ratio (MBAR) was used for the analysis of the FEP data. To obtain statistically converged results, binding energy calculations were carried out for both the forward (WT to mutant) and backward directions (mutant to WT) and the error was calculated by taking the differences between the forward and backward calculations (Figure 5).

No major difference in affinity for ATP was observed for any of these mutations over the $EGFR^{WT}$ ($\Delta\Delta G$ is with in <1 kcal/mol; Figure 6). Although the NH of the adenine motif of ATP forms an h-bond with the hydroxyl side chain of Thr790, and this interaction is lost upon various substitutions except in $EGFR^{T790S}$, the fact that no major loss in affinity was observed suggests that this *EGFR*−ATP hydrogen bond is not that critical for the binding of ATP. This is further supported by the fact that only ∼19% of the kinases from the human kinome carry a residue at this gatekeeper position that can engage in such a hydrogen bond with bound ATP. Interestingly T790M also did not show increased affinity for the ATP ($\Delta\Delta G \sim 0.2$ kcal/mol), in agreement with the experimental data which showed that T790M alone as a single mutant does not have increased affinity for ATP (Km for $EGFR^{WT}$ is 5.9 μM and for $EGFR^{T790M}$ is 5.2 μM)[20] although the mutant has been shown to exhibit a 5-fold improved kcat. In contrast, all the bound drugs showed increased affinity for all the mutants (Figure 6). This is not surprising since all three drugs are quinazoline derivatives, bind similarly in the ATP pocket and interact with the hinge region of the kinase through similar h-bond interactions.

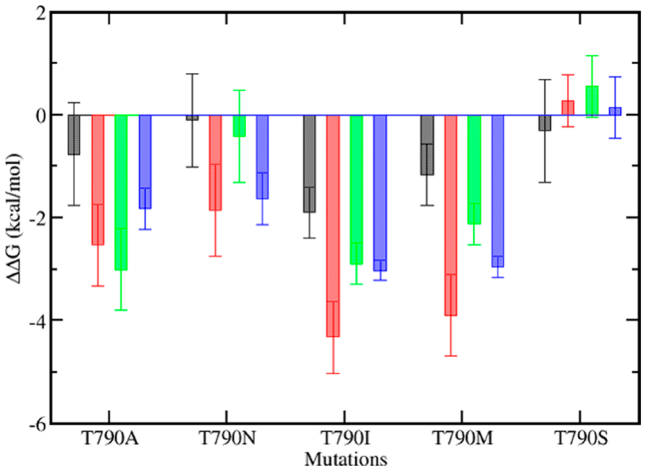

Figure 6. Free energies of mutating Thr790 to various amino acids in *EGFR* complexed to ATP (black), erlotinib (red), gefitinib (green), and afatinib (blue) calculated using FEP/MBAR. The difference between the forward (WT to Mut) and backward (Mut to WT) are shown as errors.

Surprisingly both erlotinib and gefitinib showed increased affinity (by ∼1.0 kcal/mol and ∼1.3 kcal/mol respectively) for $EGFR^{T790M}$, which contrasts with the clinical observations where this mutant is known to confer resistance to these two inhibitors. The increased affinity observed for the $EGFR^{T790M}$ for gefitinib (∼1.3 kcal/mol) is in good agreement with the experimental data on increased binding reported for the $EGFR^{T790M}$ (K_d of 4.9 nM for the $EGFR^{T790M}$ versus K_d of 54.3 nM for $EGFR^{WT}$).[20] This 10-fold increase in K_d corresponds to a binding free energy of ∼1.2 kcal/mol favoring the binding of gefitinib to $EGFR^{T790M}$ over the $EGFR^{WT}$ (Table 2). It is speculated that the $EGFR^{T790M}$ results in resistance to the drug gefitinib by increasing its binding to the natural substrate ATP.[20]

Our binding energy calculations further suggest that the other two drugs erlotinib and afatinib also show a higher affinity for $EGFR^{T790M}$, in contrast to the observation clinically that the $EGFR^{T790M}$ mutant does not bind to gefitinib and erlotinib. Of course, afatinib will bind $EGFR^{T790M}$ due to the irreversible interaction through the covalent bond with Cys797; indeed, it was designed with this hypothesis and it successfully entered the clinic for patients who have developed the $EGFR^{T790M}$ mutation.

In summary, mutations at position Thr790 including Met, Ile, Ala and to a lesser extent, Ser and Asn favor the binding of all three inhibitors whereas the binding to ATP remains relatively similar. And yet, $EGFR^{T790M}$ is most prevalent in the clinic. Incidentally, ∼37% of the kinases in the human kinome carry Met at the gatekeeper position, followed by Thr (∼19%), Leu (16%), and Phe (∼14%). In contrast, Ile, Ala, Ser, and Asn together account for only ∼4%. There is no evidence of Lys or Arg at this position, and this is consistent with our observations that the side chains occlude the pocket sufficiently to perturb the binding of ATP and abrogate function; hence, this residue will not be selected for.

CONCLUSIONS

The emergence of resistance against drugs that inhibit a particular protein/enzyme, thus disabling pathways that are essential for tumor survival is a major problem in targeted therapy. There are several routes to the development of resistance including the emergence of point mutations in the target that disable the binding of the drug or the alteration of pathways, extrusion of drugs through pumps, etc.[51] There is some hope that the recently identified allosteric inhibitors may be able to avert this problem.[52−54]

Table 2. Binding Affinity/Free Energy of Gefitinib with EGFR[a]

	K_d (nM)		ΔG (kcal/mol)		
system	$EGFR^{WT}$	$EGFR^{T790M}$	$EGFR^{WT}$	$EGFR^{T790M}$	$\Delta\Delta G$ (kcal/mol)
experimental	35.3	4.6	−10.22	−11.4	−1.21
computational					−1.3

[a] K_d is the dissociation constant of gefitinib reported by Yun et al.[20] Experimental binding free energy (ΔG) was calculated from the K_d values using $\Delta G = -RT \ln(K_d)$, where R is gas constant (0.001987 kcal/mol) and T is temperature (300 K).

DOI: 10.1021/acs.jcim.9b00361
J. Chem. Inf. Model. XXXX, XXX, XXX−XXX

An area of focus has been the development of drugs that are designed to address the issue of the emergence of point mutations in target proteins; the development of first, second, third and fourth generation drugs against kinases in oncology[55] exemplifies the need for continuous evolution of drugs. This outlines the need to understand the nature of the point mutations that will arise in response to a drug. One such example is the prevalence of the $EGFR^{T790M}$ gatekeeper mutation in *EGFR* kinase that arises in response to first line drugs. However, the reason for the prevalence of the Met mutation at the 790 position remains enigmatic, because even with a single base change at the nucleotide level (cytosine to thymine change), the possible mutations include, in addition to Met, Ala, Asn, Ile, Ser, Pro, Arg, and Lys. So why is Met the most commonly seen mutation at 790? In the current study we explore the structural and energetic consequences of a set of mutations at the 790 position upon the interactions/affinity for ATP and three commonly used drugs: the first generation erlotinib and gefitinib and the second generation afatinib. These mutations are the possible ones that result from a single base change.

The Pro mutation was discarded as it was found to be quite destabilizing in the apo state itself. The Lys and Arg mutations interfere with the binding of ATP and hence are of no functional consequence. The remaining five mutations were all found to be tolerated structurally (change in thermodynamic stabilities estimated using a set of available web servers on the kinases in their active and inactive forms), had negligible differences in their affinities for ATP compared to $EGFR^{WT}$, in accord with experimental observations,[20] and tolerated the binding of the three inhibitors. This may explain why these mutations are not seen since the protein is not "gaining" anything. In vivo of course there are the complex networks of chaperones that have evolved to modulate the stabilities of proteins;[56] however, that investigation is beyond the scope of the current study. In our calculations, only T790I (and T790M) showed increased affinity for the inhibitors compared to $EGFR^{WT}$, in accord with experimental observations for $EGFR^{T790M}$. And yet the T790M mutant is the only one seen in response to the administration of drugs (the resistance mutation). A resolution to this enigma was provided by Eck and colleagues,[20] who found that the T790M mutant can easily accommodate the tight binding of several inhibitors, as we also find in our simulations. They suggest that the high cellular concentration of ATP weakens the efficacy of the drugs for $EGFR^{T790M}$[20] and drugs such as afatinib, which belong to the same family of inhibitors as gefitinib and erlotinib, are effective simply because they can bind irreversibly to $EGFR^{T790M}$. So why do we not see the T790I mutation in the clinic as a resistance mutation. Although the current FEP/TI methods are unable to provide a conclusive answer, it is possible that kinetics of drug binding may need to be factored in, a characteristic that is increasingly being explored in drug discovery paradigms.[57,58] Of course, the current study assumes that resistance arises from point mutations in the target protein. Other factors likely play a role, as a recent study[59] highlighted how first-generation inhibitors of *EGFR* activate the NFkB pathway that in turn results in induction of activation-induced cytidine deaminase (AICDA) which deaminates a specific 5-methyl cytosine to thymine, resulting in the $EGFR^{T790M}$ mutation.

■ ASSOCIATED CONTENT

Supporting Information

The Supporting Information is available free of charge on the ACS Publications website at DOI: 10.1021/acs.jcim.9b00361.

Details of computational methods used in this study (PDF)

■ AUTHOR INFORMATION

Corresponding Authors

*E-mail: raghavk@bii.a-star.edu.sg. Tel: +65 6478 8353. Fax: +65 6478 9048.

*E-mail: chandra@bii.a-star.edu.sg. Tel: +65 6478 8273. Fax: +65 6478 9048.

ORCID

Srinivasaraghavan Kannan: 0000-0002-9539-5249

Chandra S. Verma: 0000-0003-0733-9798

Notes

The authors declare no competing financial interest.

■ ACKNOWLEDGMENTS

The authors thank National Super Computing Centre (NSCC) for computing facilities. We thank A*STAR for support; S.K. is partly funded by IAF-PP Grant H18/01/a0/015 (A*STAR/NRF/EDB); S.J.F. is funded by IAF-PP Grant H17/01/a0/0W9 (A*STAR/NRF/EDB).

■ REFERENCES

(1) Santos, R.; Ursu, O.; Gaulton, A.; Bento, A. P.; Donadi, R. S.; Bologa, C. G.; Karlsson, A.; Al-Lazikani, B.; Hersey, A.; Oprea, T. I.; Overington, J. P. A Comprehensive Map of Molecular Drug Targets. *Nat. Rev. Drug Discovery* **2017**, *16*, 19−34.

(2) Fabbro, D.; Cowan-Jacob, S. W.; Moebitz, H. Ten Things you should know about Protein Kinases: IUPHAR review 14. *Br. J. Pharmacol.* **2015**, *172*, 2675−2700.

(3) Fabbro, D. 25 Years of Small Molecular Weight Kinase Inhibitors: Potentials and Limitations. *Mol. Pharmacol.* **2015**, *87*, 766−775.

(4) Roskoski, R., Jr. A Historical Overview of Protein Kinases and their Targeted Small Molecule Inhibitors. *Pharmacol. Res.* **2015**, *100*, 1−23.

(5) Klaeger, S.; Heinzlmeir, S.; Wilhelm, M.; Polzer, H.; Vick, B.; Koenig, P. A.; Reinecke, M.; Ruprecht, B.; Petzoldt, S.; Meng, C.; Zecha, J.; Reiter, K.; Qiao, H.; Helm, D.; Koch, H.; Schoof, M.; Canevari, G.; Casale, E.; Depaolini, S. R.; Feuchtinger, A.; Wu, Z.; Schmidt, T.; Rueckert, L.; Becker, W.; Huenges, J.; Garz, A. K.; Gohlke, B. O.; Zolg, D. P.; Kayser, G.; Vooder, T.; Preissner, R.; Hahne, H.; Tõnisson, N.; Kramer, K.; Götze, K.; Bassermann, F.; Schlegl, J.; Ehrlich, H. C.; Aiche, S.; Walch, A.; Greif, P. A.; Schneider, S.; Felder, E. R.; Ruland, J.; Médard, G.; Jeremias, I.; Spiekermann, K.; Kuster, B. The Target Landscape of Clinical Kinase Drugs. *Science* **2017**, *358*, 6367.

(6) Wu, P.; Nielsen, T. E.; Clausen, M. H. Small-Molecule Kinase Inhibitors: An Analysis of FDA-approved Drugs. *Drug Discovery Today* **2016**, *21*, 5−10.

(7) Barouch-Bentov, R.; Sauer, K. Mechanisms of Drug Resistance in Kinases. *Expert Opin. Invest. Drugs* **2011**, *20*, 153−208.

(8) Lovly, C. M.; Shaw, A. T. Molecular Pathways: Resistance to Kinase Inhibitors and Implications for Therapeutic Strategies. *Clin. Cancer Res.* **2014**, *20*, 2249−2256.

(9) Chen, Y. F.; Fi, Lw. Mechanisms of Acquired Resistance to Tyrosine Kinase Inhibitors. *Acta Pharm. Sin. B* **2011**, *1*, 197−207.

(10) Rosenzweig, S. T. Acquired Resistance to Drugs Targeting Tyrosine Kinases. *Adv. Cancer Res.* **2018**, *138*, 71−98.

DOI: 10.1021/acs.jcim.9b00361
J. Chem. Inf. Model. XXXX, XXX, XXX−XXX

(11) Azam, M.; Latek, R. R.; Daley, G. Q. Mechanisms of Autoinhibition and STI-571/imatinib Resistance Revealed by Mutagenesis of BCR-ABL. *Cell* **2003**, *112*, 831−843.
(12) Weisberg, E.; Manley, P. W.; Cowan-Jacob, S. W.; Hochhaus, A.; Griffin, J. D. Second Generation Inhibitors of BCR-ABL for the Treatment of Imatinib-resistant Chronic Myeloid Leukaemia. *Nat. Rev. Cancer* **2007**, *7*, 345−356.
(13) Azam, M.; Seeliger, M. A.; Gray, N. S.; Kuriyan, J.; Daley, G. Q. Activation of Tyrosine Kinases by Mutation of the Gatekeeper Threonine. *Nat. Struct. Mol. Biol.* **2008**, *15*, 1109−1118.
(14) Kornev, A. P.; Haste, N. M.; Taylor, S. S.; Eyck, L. F. Surface Comparison of Active and Inactive Protein Kinases Identifies a Conserved Activation Mechanism. *Proc. Natl. Acad. Sci. U. S. A.* **2006**, *103*, 17783−17788.
(15) Gibbons, D. L.; Pricl, S.; Kantarjian, H.; Cortes, J.; Quintás-Cardama, A. The Rise and Fall of Gatekeeper Mutations? The BCR-ABL1 T315I paradigm. *Cancer* **2012**, *118*, 293−299.
(16) Wang, Z.; Chen, R.; Wang, S.; Zhong, J.; Wu, M.; Zhao, J.; Duan, J.; Zhuo, M.; An, T.; Wang, Y.; Bai, H.; Wang, J. Quantification and Dynamic Monitoring of EGFR T790M in Plasma Cell-free DNA by Digital PCR for Prognosis of EGFR-TKI Treatment in Advanced NSCLC. *PLoS One* **2014**, *9* (11), No. e110780.
(17) Heinrich, M. C.; Corless, C. L.; Blanke, C. D.; Demetri, G. D.; Joensuu, H.; Roberts, P. J.; Eisenberg, B. L.; von Mehren, M.; Fletcher, C. D.; Sandau, K.; McDougall, K.; Ou, W. B.; Chen, C. J.; Fletcher, J. A. Molecular Correlates of Imatinib Resistance in Gastrointestinal Stromal Tumors. *J. Clin. Oncol.* **2006**, *24*, 4764−4774.
(18) Metzgeroth, G.; Erben, P.; Martin, H.; Mousset, S.; Teichmann, M.; Walz, C.; Klippstein, T.; Hochhaus, A.; Cross, N. C. P.; Hofmann, W.-K.; Reiter, A. Limited Clinical Activity of Nilotinib and Sorafenib in FIP1L1-PDGFRA Positive Chronic Eosinophilic Leukemia with Imatinib-resistant T674I Mutation. *Leukemia* **2012**, *26*, 162−164.
(19) Pauwels, D.; Sweron, B.; Cools, J. The N676D and G697R Mutations in the Kinase Domain of FLT3 Confer Resistance to the Inhibitor AC220. *Haematologica.* **2012**, *97*, 1773−1774.
(20) Yun, C. H.; Mengwasser, K. E.; Toms, A. V.; Woo, M. S.; Greulich, H.; Wong, K. K.; Meyerson, M.; Eck, M. J. The T790M Mutation in EGFR Kinase Causes Drug Resistance by Increasing the Affinity for ATP. *Proc. Natl. Acad. Sci. U. S. A.* **2008**, *105*, 2070−2075.
(21) Shan, Y.; Eastwood, M. P.; Zhang, X.; Kim, E. T.; Arkhipov, A.; Dror, R. O.; Jumper, J.; Kuriyan, J.; Shaw, D. E. Oncogenic Mutations Counteract Intrinsic Disorder in the EGFR Kinase and Promote Receptor Dimerization. *Cell* **2012**, *149*, 860−870.
(22) Sutto, L.; Gervasio, F. L. Effects of Oncogenic Mutations on the Conformational Free-Energy Landscape of EGFR Kinase. *Proc. Natl. Acad. Sci. U. S. A.* **2013**, *110*, 10616−10621.
(23) Kornev, A. P.; Haste, N. M.; Taylor, S. S.; Eyck, L. F. Surface Comparison of Active and Inactive Protein Kinases Identifies a Conserved Activation Mechanism. *Proc. Natl. Acad. Sci. U. S. A.* **2006**, *103*, 17783−17788.
(24) Azam, M.; Seeliger, M. A.; Gray, N. S.; Kuriyan, J.; Daley, G. Q. Activation of Tyrosine Kinases by Mutation of the Gatekeeper Threonine. *Nat. Struct. Mol. Biol.* **2008**, *15*, 1109−1118.
(25) Tsai, C. J.; Nussinov, R. The Free Energy Landscape in Translational Science: how can Somatic Mutations Result in Constitutive Oncogenic Activation? *Phys. Chem. Chem. Phys.* **2014**, *16*, 6332−6341.
(26) Kannan, S.; Pradhan, M. R.; Tiwari, G.; Tan, W. C.; Chowbay, B.; Tan, E. H.; Tan, D. S.; Verma, C. Hydration Effects on the Efficacy of the Epidermal Growth Factor Receptor Kinase Inhibitor Afatinib. *Sci. Rep.* **2017**, *7*, 1540.
(27) Case, D. A.; Ben-Shalom, I. Y.; Brozell, S. R.; Cerutti, D. S.; Cheatham, T. E., III; Cruzeiro, V. W. D.; Darden, T. A.; Duke, R. E.; Ghoreishi, D.; Gilson, M. K.; Gohlke, H.; Goetz, A. W.; Greene, D.; Harris, R.; Homeyer, N.; Izadi, S.; Kovalenko, A.; Kurtzman, T.; Lee, T. S.; LeGrand, S.; Li, P.; Lin, C.; Liu, J.; Luchko, T.; Luo, R.; Mermelstein, D. J.; Merz, K. M.; Miao, Y.; Monard, G.; Nguyen, C.; Nguyen, H.; Omelyan, I.; Onufriev, A.; Pan, F.; Qi, R.; Roe, D. R.; Roitberg, A.; Sagui, C.; Schott-Verdugo, S.; Shen, J.; Simmerling, C. L.; Smith, J.; Salomon-Ferrer, R.; Swails, J.; Walker, R. C.; Wang, J.; Wei, H.; Wolf, R. M.; Wu, X.; Xiao, L.; York, D. M.; Kollman, P. A. *AMBER 16*; University of California: San Francisco, CA, 2016.
(28) Maier, J. A.; Martinez, C.; Kasavajhala, K.; Wickstrom, L.; Hauser, K. E.; Simmerling, C. ff14SB: Improving the Accuracy of Protein Side Chain and Backbone Parameters from ff99SB. *J. Chem. Theory Comput.* **2015**, *11*, 3696−3713.
(29) Wang, J.; Wolf, R. M.; Caldwell, J. W.; Kollman, P. A.; Case, D. A. Development and Testing of a General Amber Force Field. *J. Comput. Chem.* **2004**, *25*, 1157−1174.
(30) Kannan, S.; Tan, D. S.; Verma, C. S. Effects of Single Nucleotide Polymorphisms on the Binding of Afatinib to EGFR: A Potential Patient Stratification Factor Revealed by Modeling Studies. *J. Chem. Inf. Model.* **2019**, *59*, 309−315.
(31) Pires, D. E.; Ascher, D. B.; Blundell, T. L. DUET: a Server for Predicting Effects of Mutations on Protein Stability using an Integrated Computational Approach. *Nucleic Acids Res.* **2014**, *42*, W314−W319.
(32) Pandurangan, A. P.; Ochoa-Montano, B.; Ascher, D. B.; Blundell, T. L. SDM: a Server for Predicting Effects of Mutations on Protein Stability. *Nucleic Acids Res.* **2017**, *45*, W229−W235.
(33) Pires, D. E.; Ascher, D. B.; Blundell, T. L. mCSM: Predicting the Effects of Mutations in Proteins using Graph-Based Signatures. *Bioinformatics* **2014**, *30*, 335−342.
(34) Rodrigues, C. H.; Pires, D. E.; Ascher, D. B. DynaMut: Predicting the Impact of Mutations on Protein Conformation, Flexibility and Stability. *Nucleic Acids Res.* **2018**, *46*, W350−W355.
(35) Chen, C.; Lin, J.; Chu, Y. iStable: Off-the-shelf Predictor Integration for Predicting Protein Stability Changes. *BMC Bioinformatics* **2012**, *14*, S5.
(36) Johnson, L. N.; Noble, M. E.; Owen, D. Active and Inactive Protein Kinases: Structural Basis for Regulation. *Cell* **1996**, *85*, 149−158.
(37) Huse, M.; Kuriyan, J. The Conformational Plasticity of Protein Kinases. *Cell* **2002**, *109*, 275−282.
(38) Wang, L.; Wu, Y.; Deng, Y.; Kim, B.; Pierce, L.; Krilov, G.; Lupyan, D.; Robinson, S.; Dahlgren, M. K.; Greenwood, J.; Romero, D. L.; Masse, C.; Knight, J. L.; Steinbrecher, T.; Beuming, T.; Damm, W.; Harder, E.; Sherman, W.; Brewer, M.; Wester, R.; Murcko, M.; Frye, L.; Farid, R.; Lin, T.; Mobley, D. L.; Jorgensen, W. L.; Berne, B. J.; Friesner, R. A.; Abel, R. Accurate and Reliable Prediction of Relative Ligand Binding Potency in Prospective Drug Discovery by way of a Modern Free-energy Calculation Protocol and Force Field. *J. Am. Chem. Soc.* **2015**, *137*, 2695−2703.
(39) Clark, A. J.; Gindin, T.; Zhang, B.; Wang, L.; Abel, R.; Murret, C. S.; Xu, F.; Bao, A.; Lu, N. J.; Zhou, T.; Kwong, P. D.; Shapiro, L.; Honig, B.; Friesner, R. A. Free Energy Perturbation Calculation of Relative Binding Free Energy between Broadly Neutralizing Antibodies and the gp120 Glycoprotein of HIV-1. *J. Mol. Biol.* **2017**, *429*, 930−947.
(40) Steinbrecher, T.; Abel, R.; Clark, A.; Friesner, R. Free Energy Perturbation Calculations of the Thermodynamics of Protein Side-Chain Mutations. *J. Mol. Biol.* **2017**, *429*, 923−929.
(41) Steinbrecher, T.; Zhu, C.; Wang, L.; Abel, R.; Negron, C.; Pearlman, D.; Feyfant, E.; Duan, J.; Sherman, W. Predicting the Effect of Amino Acid Single-Point Mutations on Protein Stability—Large-Scale Validation of MD-Based Relative Free Energy Calculations. *J. Mol. Biol.* **2017**, *429*, 948−963.
(42) Lai, P. K.; Kaznessis, Y. N. Free Energy Calculations of Microcin J25 Variants Binding to the FhuA Receptor. *J. Chem. Theory Comput.* **2017**, *13*, 3413−3423.
(43) Lee, T. S.; Hu, Y.; Sherborne, B.; Guo, Z.; York, D. M. Toward Fast and Accurate Binding Affinity Prediction with pmemdGTI: An Efficient Implementation of GPU-Accelerated Thermodynamic Integration. *J. Chem. Theory Comput.* **2017**, *13*, 3077−3084.
(44) Zhu, S.; Travis, S. M.; Elcock, A. H. Accurate Calculation of Mutational Effects on the Thermodynamics of Inhibitor Binding to

DOI: 10.1021/acs.jcim.9b00361
J. Chem. Inf. Model. XXXX, XXX, XXX−XXX

p38α MAP Kinase: A Combined Computational and Experimental Study. *J. Chem. Theory Comput.* **2013**, *9*, 3151−3164.
(45) Park, J.; McDonald, J. J.; Petter, R. C.; Houk, K. N. Molecular Dynamics Analysis of Binding of Kinase Inhibitors to WT EGFR and the T790M Mutant. *J. Chem. Theory Comput.* **2016**, *12*, 2066−2078.
(46) Wang, L.; Berne, B. J.; Friesner, R. A. On Achieving High Accuracy and Reliability in the Calculation of Relative Protein−ligand Binding Affinities. *Proc. Natl. Acad. Sci. U. S. A.* **2012**, *109*, 1937−1942.
(47) Jiang, W.; Hodoscek, M.; Roux, B. Computation of Absolute Hydration and Binding Free Energy with Free Energy Perturbation Distributed Replica-Exchange Molecular Dynamics (FEP/REMD). *J. Chem. Theory Comput.* **2009**, *5*, 2583−2588.
(48) Khavrutskii, I. V.; Wallqvist, A. Computing Relative Free Energies of Solvation Using Single Reference Thermodynamic Integration Augmented with Hamiltonian Replica Exchange. *J. Chem. Theory Comput.* **2010**, *6*, 3427−3441.
(49) König, G.; Boresch, S. Non-Boltzmann Sampling and Bennett's Acceptance Ratio Method: How to Profit from Bending the Rules. *J. Comput. Chem.* **2011**, *32*, 1082−1090.
(50) Mikulskis, P.; Genheden, S.; Ryde, U. A Large-scale Test of Free-energy Simulation Estimates of Protein-ligand Binding Affinities. *J. Chem. Inf. Model.* **2014**, *54*, 2794−2806.
(51) Holohan, C.; Van Schaeybroeck, S.; Longley, D. B.; Johnston, P. G. Cancer Drug Resistance: an Evolving Paradigm. *Nat. Rev. Cancer* **2013**, *13*, 714−726.
(52) Ferraro, M.; D'Annessa, I.; Moroni, E.; Morra, G.; Paladino, A.; Rinaldi, S.; Compostella, F.; Colombo, G. Allosteric Modulators of HSP90 and HSP70: Dynamics Meets Function through Structure-Based Drug Design. *J. Med. Chem.* **2019**, *62*, 60−87.
(53) Paladino, A.; Marchetti, F.; Ponzoni, L.; Colombo, G. The Interplay between Structural Stability and Plasticity Determines Mutation Profiles and Chaperone Dependence in Protein Kinases. *J. Chem. Theory Comput.* **2018**, *14*, 1059−1070.
(54) Jia, Y.; et al. Overcoming EGFR(T790M) and EGFR(C797S) Resistance with Mutant-Selective Allosteric Inhibitors. *Nature* **2016**, *534*, 129−132.
(55) Sullivan, I.; Planchard, D. Next-Generation EGFR Tyrosine Kinase Inhibitors for Treating EGFR-Mutant Lung Cancer beyond First Line. *Front. Med.* **2017**, *3*, 76.
(56) Taipale, M.; Tucker, G.; Peng, J.; Krykbaeva, I.; Lin, Z. Y.; Larsen, B.; Choi, H.; Berger, B.; Gingras, A. C.; Lindquist, S. A Quantitative Chaperone Interaction Network Reveals the Architecture of Cellular Protein Homeostasis Pathways. *Cell* **2014**, *158*, 434−448.
(57) De Vivo, M.; Masetti, M.; Bottegoni, G.; Cavalli, A. Role of Molecular Dynamics and Related Methods in Drug Discovery. *J. Med. Chem.* **2016**, *59*, 4035−4061.
(58) Neil, B.; Ganotra, G. K.; Kokh, D. B.; Sadiq, S. K.; Wade, R. C. New Approaches for Computing Ligand−Receptor Binding Kinetics. *Curr. Opin. Struct. Biol.* **2018**, *49*, 1−10.
(59) Kadi, N. E.; Wang, L.; Davis, A.; Korkaya, H.; Cooke, A.; Vadnala, V.; Brown, N. A.; Betz, B. L.; Cascalho, M.; Kalemkerian, G. P.; Hassan, K. A. The EGFR T790M Mutation Is Acquired through AICDA-Mediated Deamination of 5-Methylcytosine following TKI Treatment in Lung Cancer. *Cancer Res.* **2018**, *78*, 6728−6735.

DOI: 10.1021/acs.jcim.9b00361
J. Chem. Inf. Model. XXXX, XXX, XXX−XXX